Supporting information files

Hydroxyl Deficiency-Induced Mixed Linkages in Covalent Pyrimidine Frameworks towards Enhancing Stability during H_2O_2 Photosynthesis

Yongxia Li[a*] Jingyang Zhang,[b] Xingyu Zhang,[a] Wenbo Li [a] and Aiguo Kong[b*]

[a] Department of Chemistry, Xinzhou Normal University, Xinzhou 034000, China

[b] School of Chemistry and Molecular Engineering, East China Normal University, Shanghai 200241, P. R. China

*Corresponding authors. E-mail: agkong@chem.ecnu.edu.cn; yxli@xztu.edu.cn

In-situ infrared Fourier transform spectroscopy

The O_2 atmosphere containing with H_2O vapor was firstly bubbling into in-situ infrared cell with COFs, and the FT-IR signals in the dark were collected at 5, 15 and 30 min for observing the adsorption of O_2 and H_2O on COFs. After that, the visible light was turned on, and the FT-IR spectra during photocatalysis were recorded under the presence of H_2O and O_2 at given times.

Isotope labelling experiments

2 mg of catalysts and 0.5 mL of $H_2{}^{18}O$ (97%) were put in a sealed quartz vial (5 mL). Then, the suspension was obtained by ultrasonication. Pure N_2 was bubbled into the suspension for 30 min in the dark. After 2 h irradiation, the gas products in the headspace of the reaction vessel were collected and analyzed by GC-MS (GCMS-QP2010 SE, SHIMADZU).

The apparent quantum yield (AQY) measurements.

The AQY of H_2O_2 photosynthesis in the similar conditions with 50 mg catalyst was tested under 400 nm band-pass filter by the following equation:

$$AQY = \frac{2 \times n_{H_2O_2} \times N_A \times \frac{h \cdot c}{\lambda}}{P_{\text{incident}} \times \Delta t}$$

Where $N_A = 6.02\times10^{23}$, h = 6.626×10^{-34} J s, c = 3×10^{8} m s^{-1}, The light intensity was determined with a radiometer (Perfect Light, PL-MW2000).

Theoretical calculations.

The Vienna Ab Initio Package (VASP) was employed to perform all the density functional theory (DFT) calculations within the generalized gradient approximation (GGA) using the Perdew, Burke, and Enzerhof (PBE) formulation.[1-3] The projected augmented wave (PAW) potentials were applied to describe the ionic cores and take valence electrons into account using a plane wave basis set with a kinetic energy cutoff

of 450 eV.[4,5] Partial occupancies of the Kohn–Sham orbitals were allowed using the Gaussian smearing method and a width of 0.05 eV. The electronic energy was considered self-consistent when the energy change was smaller than 10^{-5} eV. A geometry optimization was considered convergent when the force change was smaller than 0.05 eV/Å. Grimme's DFT-D3 methodology was used to describe the dispersion interactions.[6] The vacuum spacing perpendicular to the plane of the structure is 20 Å. The Brillouin zone integral utilized the surfaces structures of 1×1×1 monkhorst pack K-point sampling. Finally, the adsorption energies (E_{ads}) were calculated as Eads= $E_{ads/sub}$-E_{ads}-E_{sub}, where $E_{ad/sub}$, E_{ad}, and E_{sub} are the total energies of the optimized adsorbate/substrate system, the adsorbate in the structure, and the clean substrate, respectively.

The free energy was calculated using the equation:

$$G=E_{ads}+ZPE-TS$$

where G, Eads, ZPE and TS are the free energy, total energy from DFT calculations, zero point energy and entropic contributions, respectively.

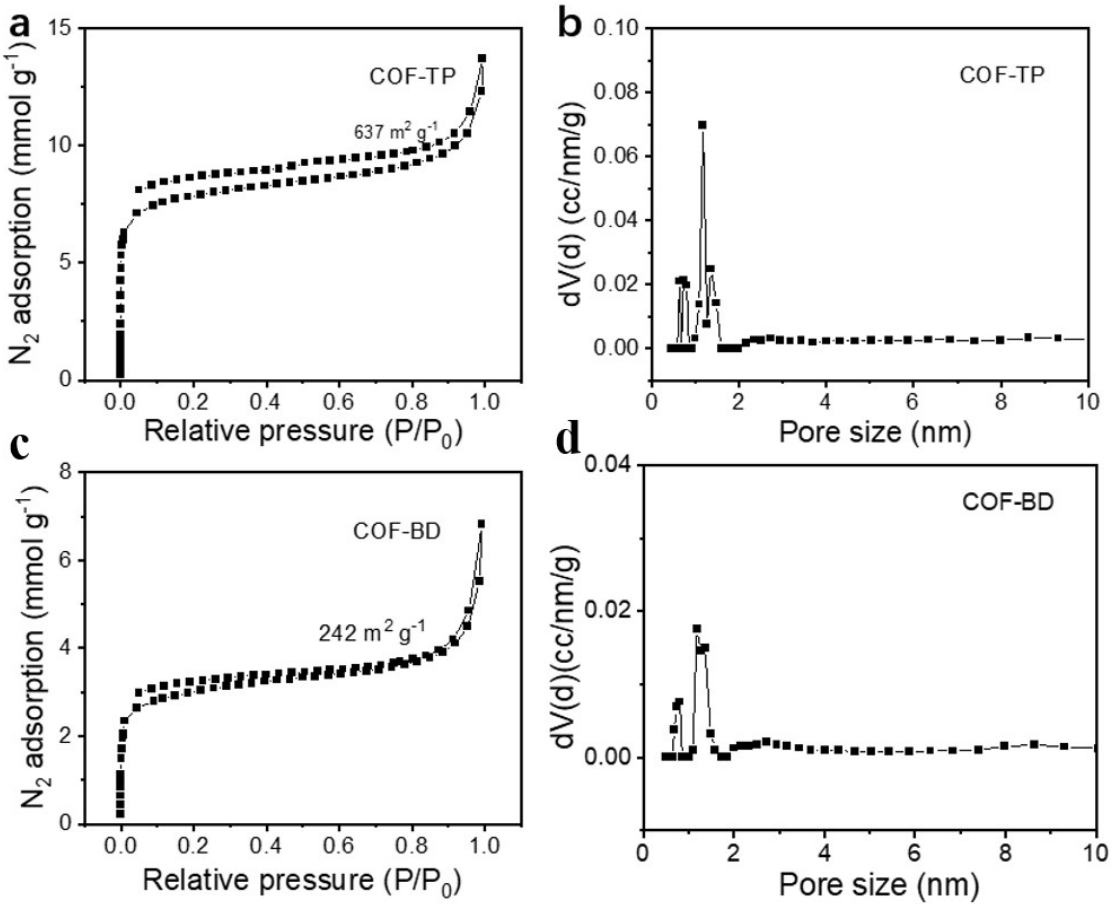

Figure S1 (a and b) The N_2 sorption isotherm (a) and the pore size distribution curve based on NLDFT model (b) for COF-TP. (c and d) The N_2 sorption isotherm (c) and the pore size distribution curve based on NLDFT model (d) for COF-BD.

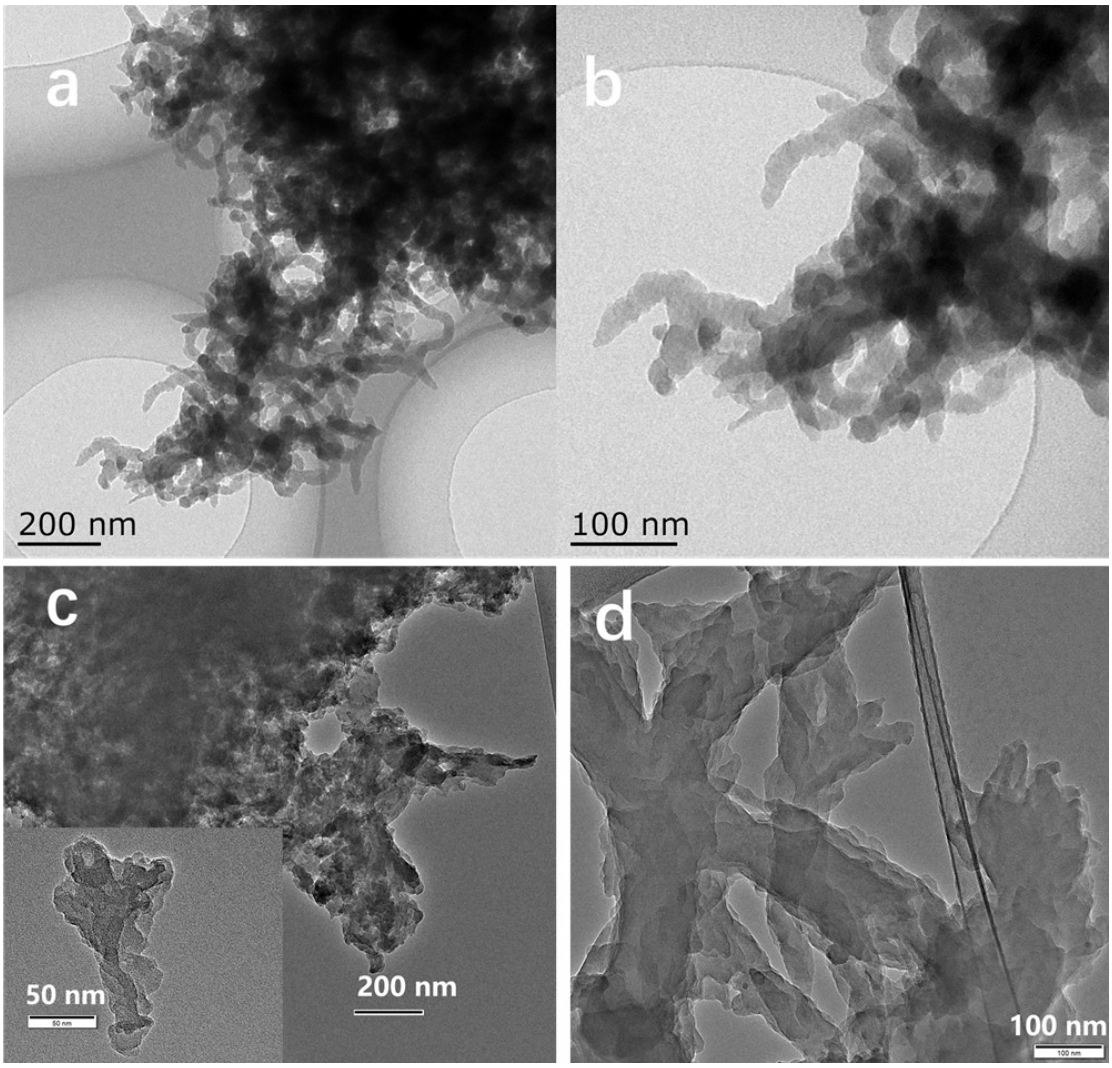

Figure S2 TEM images of COF-TP (a and b) and the corresponding TEM images of the residual COF-TP after irradiation (c and d)

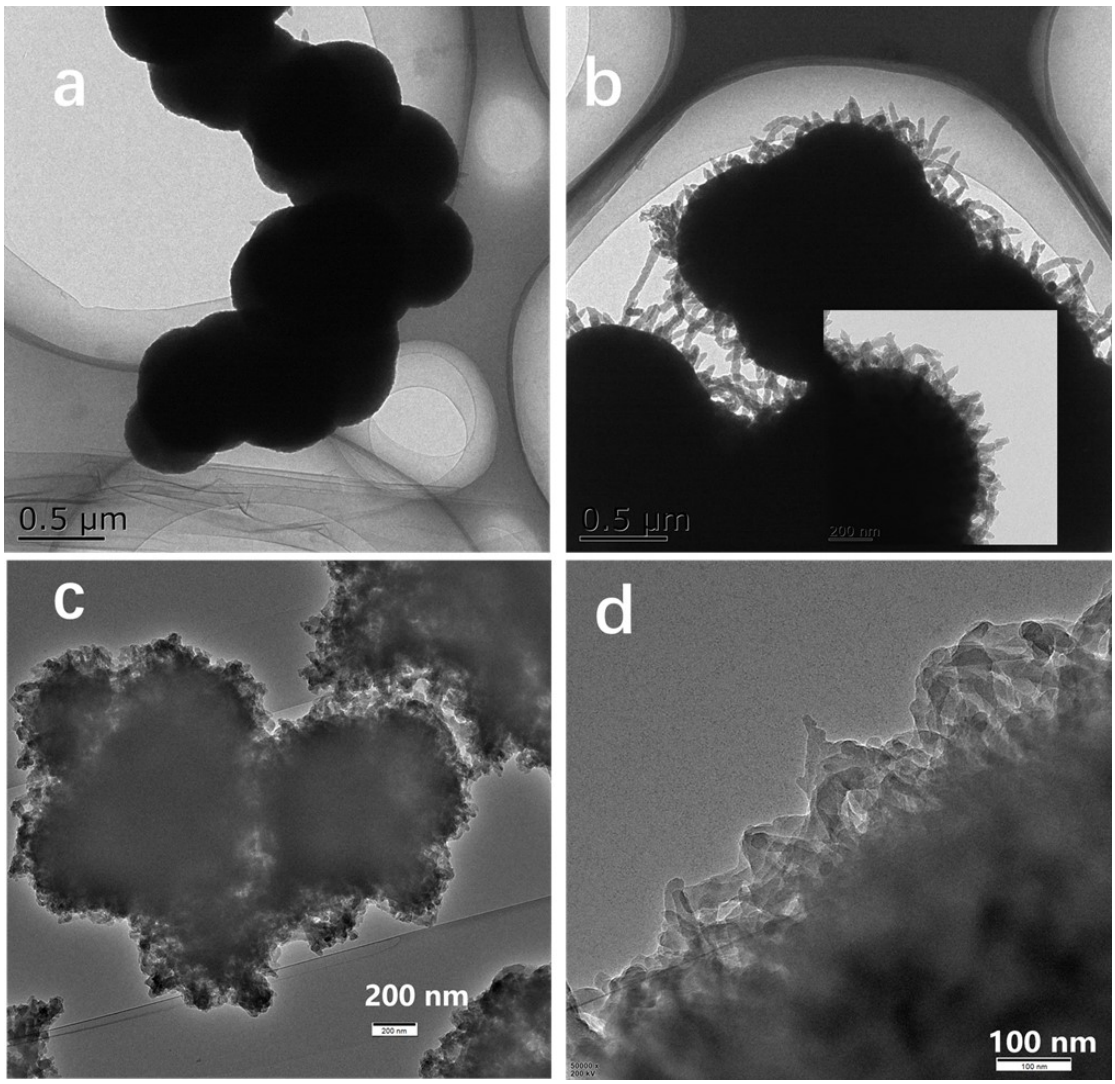

Figure S3 TEM images of COF-BD (a and b) and the corresponding TEM images of the collected COF-BD samples after irradiation (c and d)

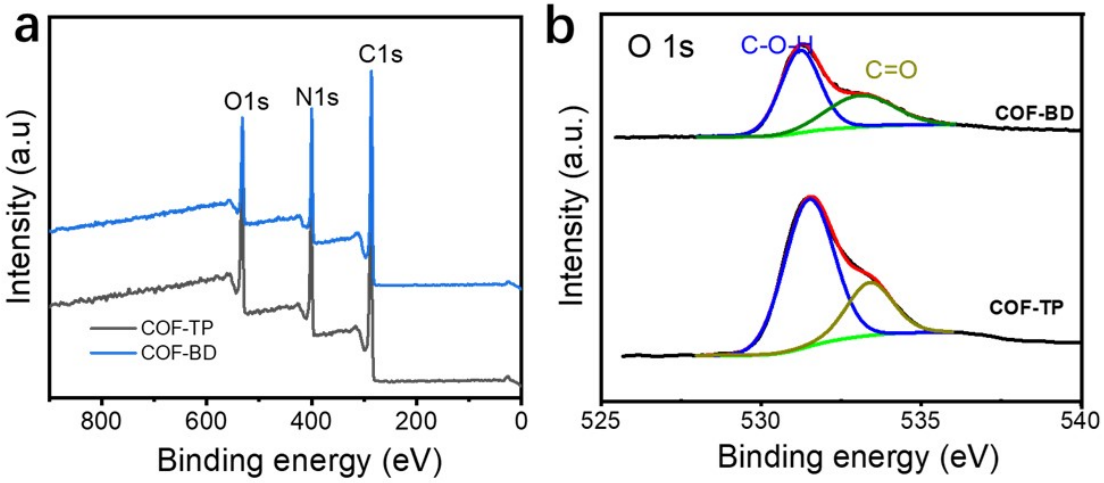

Figure S4 (a) XPS survey spectra of COF-TP and COF-BD. (b) High-resolution O1s XPS spectra of COF-TP and COF-BD

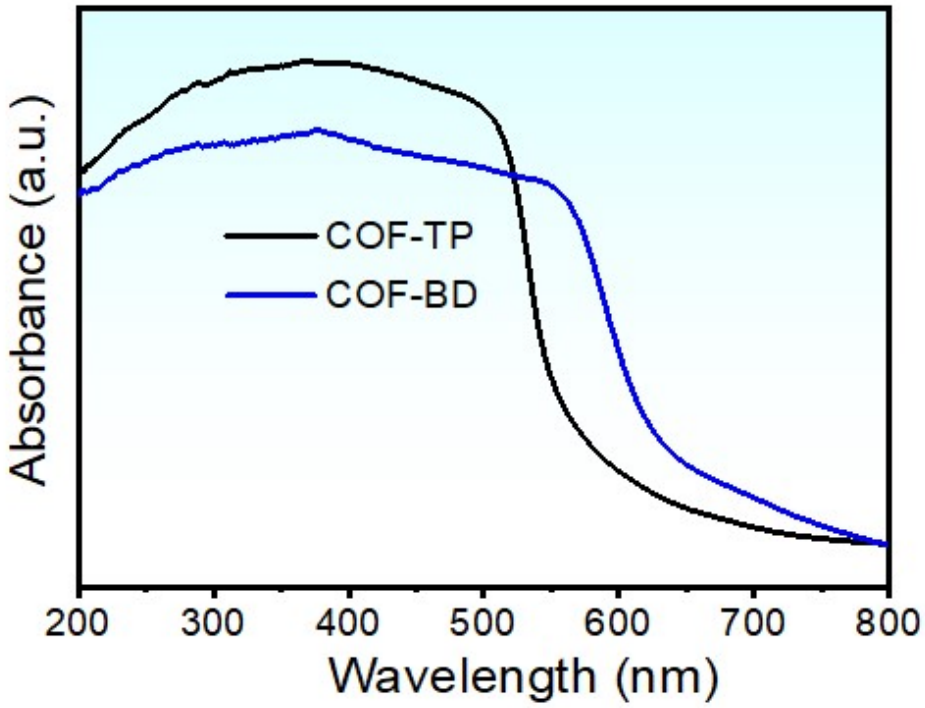

Figure S5 The UV−vis DRS curves for COF-TP and COF-BD

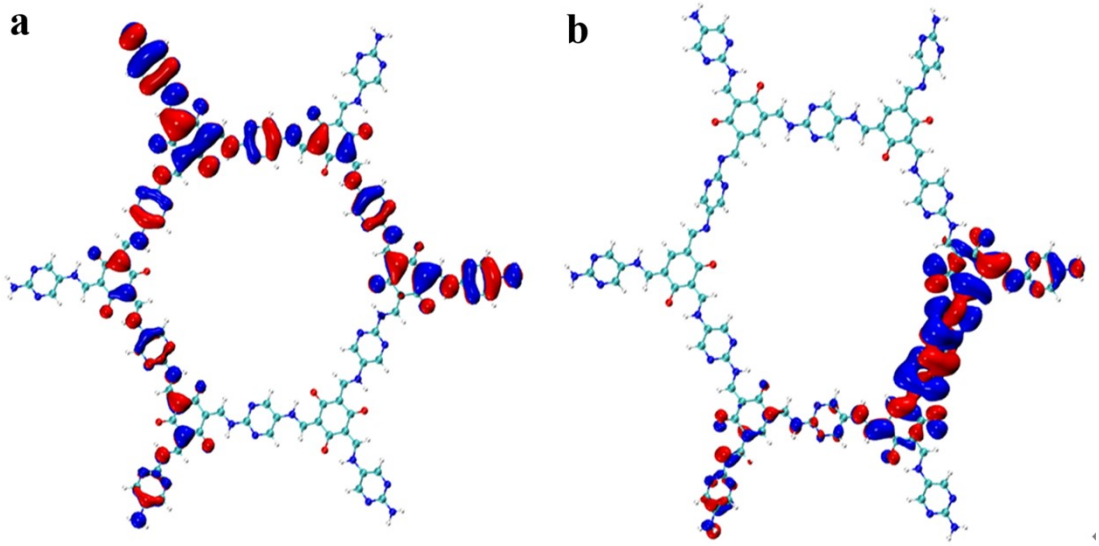

Figure S6 The calculated LUMO orbit distributions of COF-TP (a) and COF-BD (b)

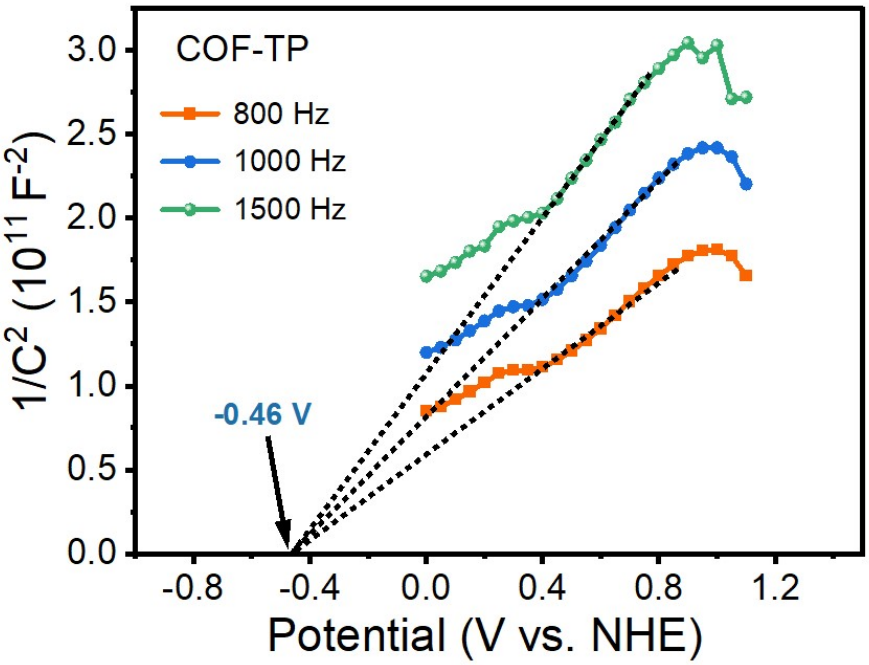

Figure S7 The Mott-Scotty plots of COF-TP in 0.1 M Na_2SO_4 electrolyte.

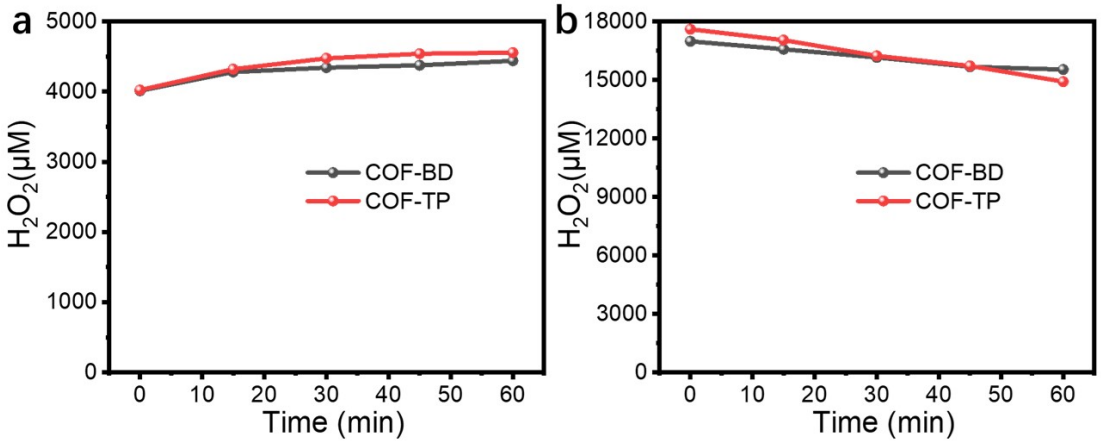

Figure S8 (a and b) H_2O_2 decomposition curves on COF-BD and COF-TP. Reaction conditions: 5 mg catalyst, 40 mL H_2O_2 solution of about 4000 μM (a) or about 17000 μM(b), visible light > 420 nm and room temperature.

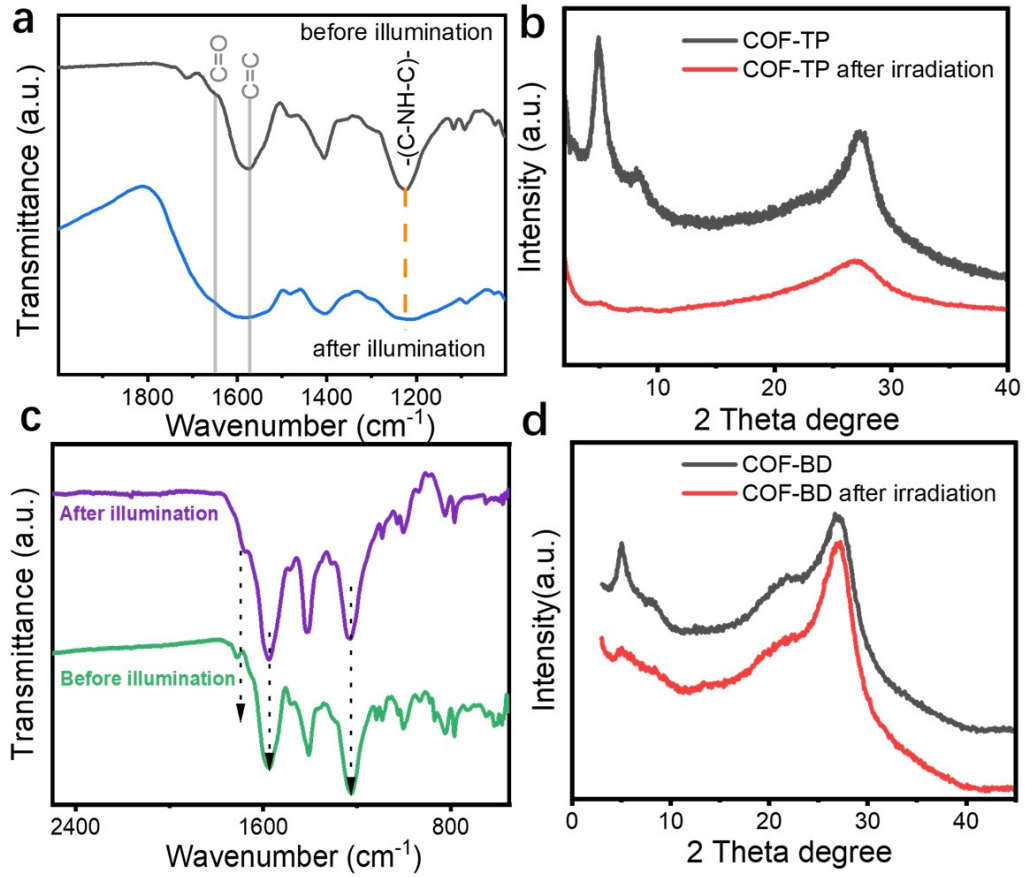

Figure S9 FT-IR spectra (a and c) and PXRD patterns (b and d) of COF-TP (a and b) and COF-BD (c and d) before and after undergoing irradiation

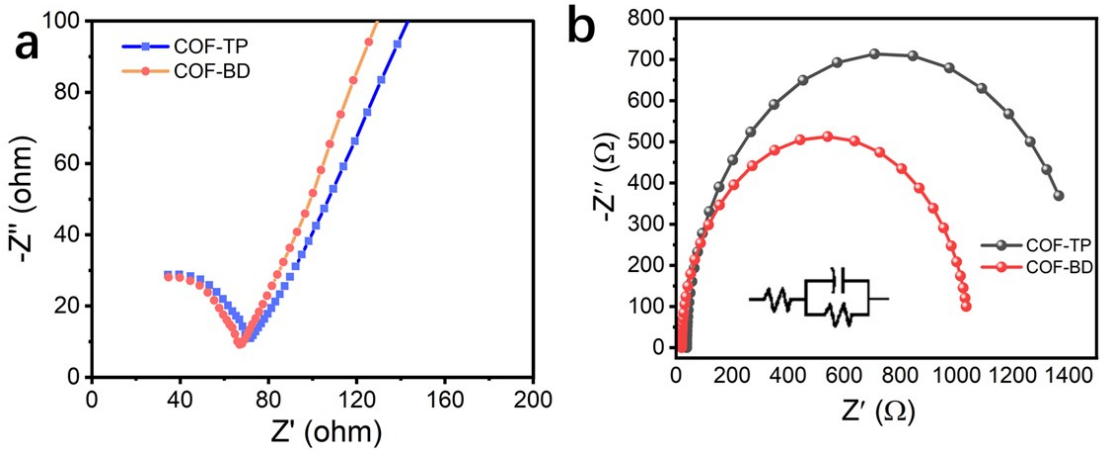

Figure S10 The original EIS spectra of COF-TP and COF-BD and the corresponding simulated EIS curves according to the inset equivalent circuit.

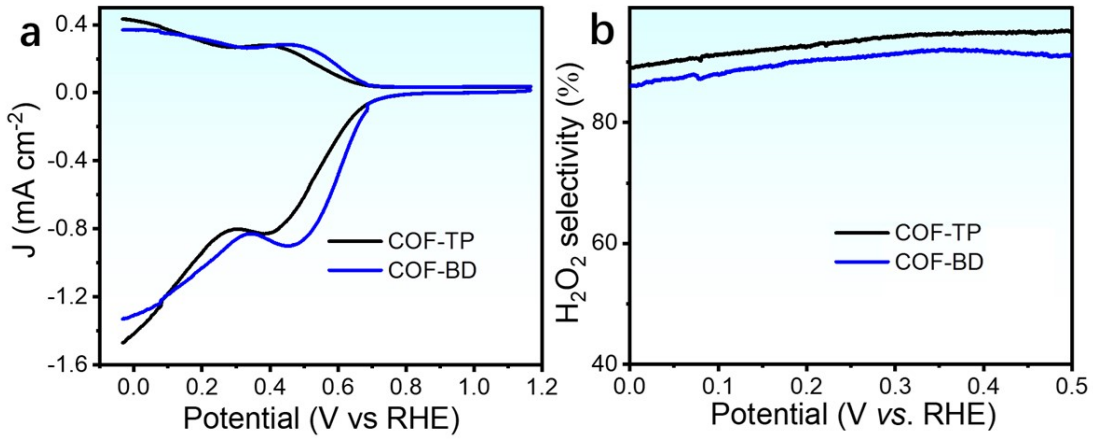

Figure S11 The ORR LSV curves (a) and H_2O_2 selectivity (b) in 0.1 M PBS for COF-TP and COF-BD

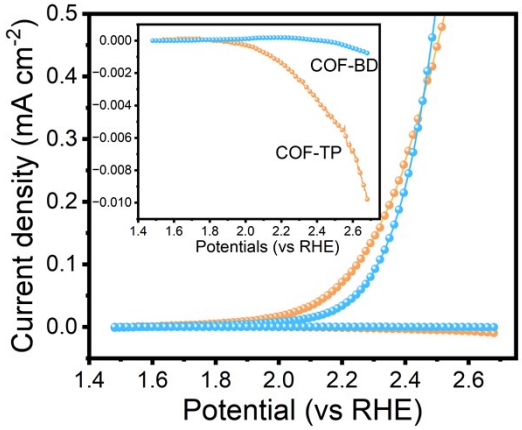

Figure S12 The WOR LSV curves on the RRDE electrode in 0.1 M Na_2SO_4. Inset is the enlarged current density on ring electrode.

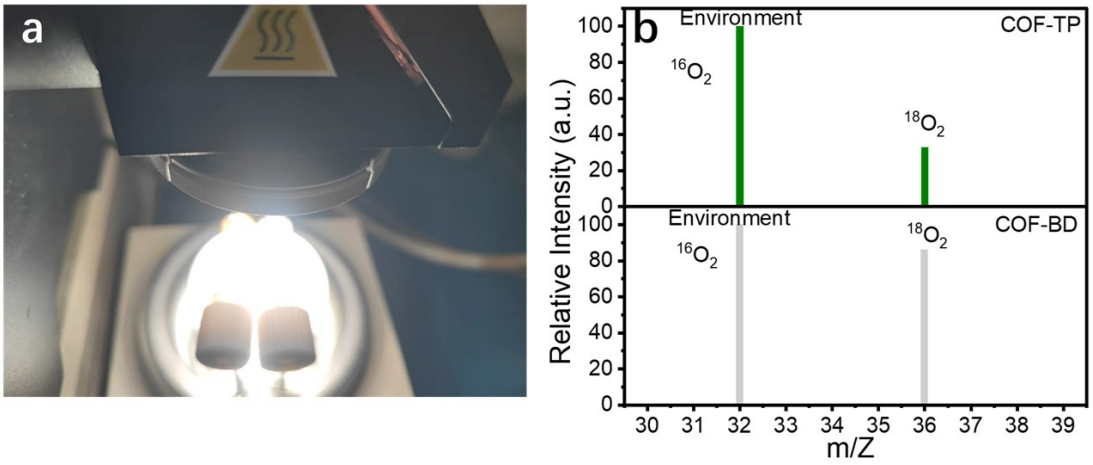

Figure S13 ^{18}O isotope labeling experiment conducted in N_2-saturated $H_2{}^{18}O$ solution and the corresponding GC-MS results

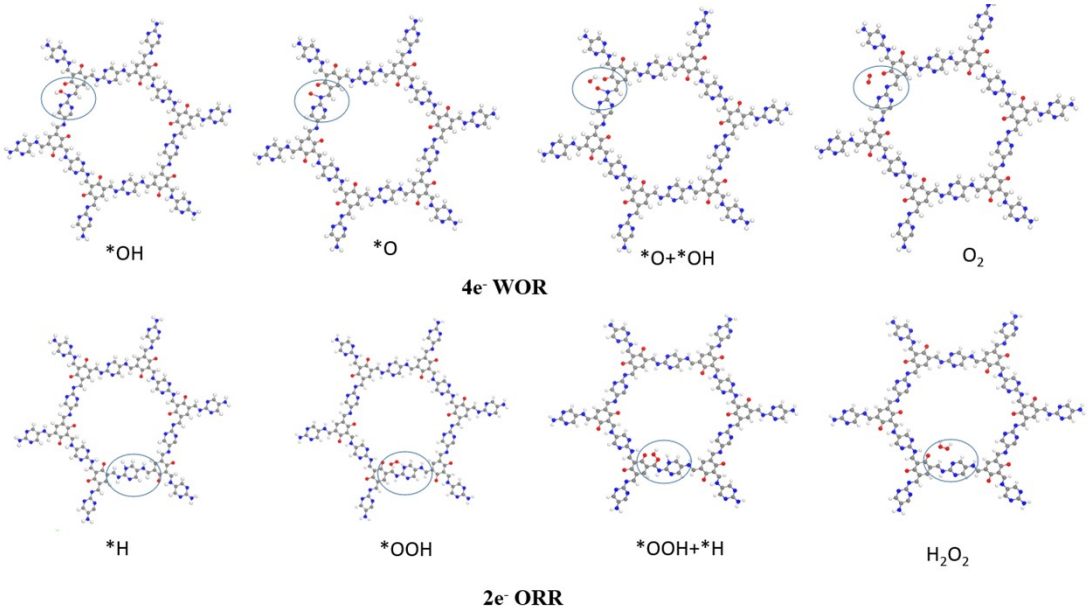

Figure S14 Optimized structure snapshots of key reaction intermediates in $2e^-$ ORR and $4e^-$ WOR on COF-BD.

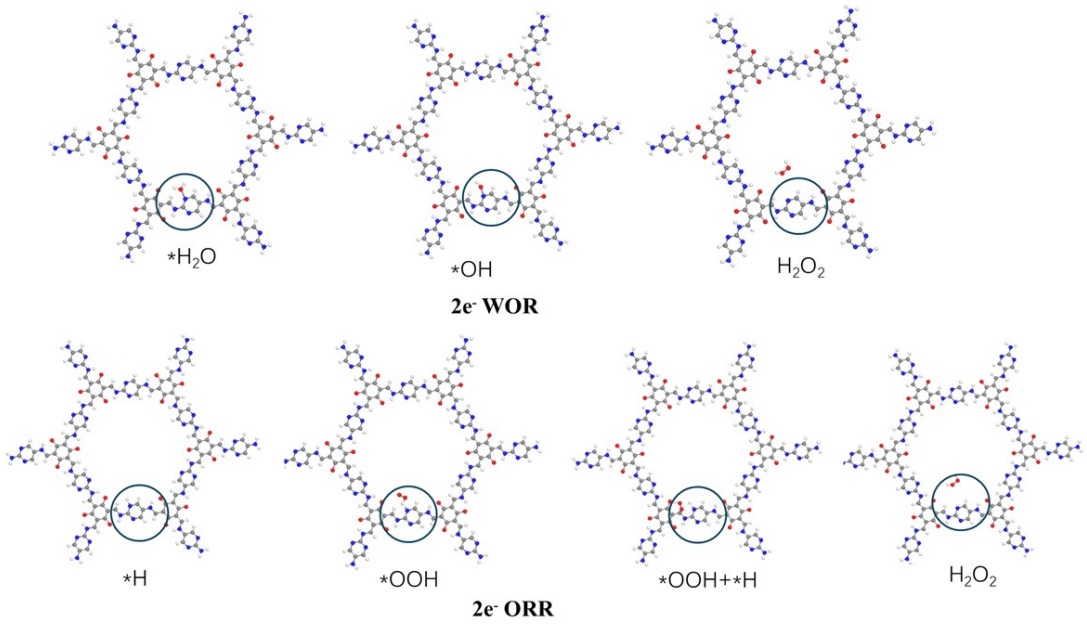

Figure S15 Optimized structure snapshots of key reaction intermediates in 2e⁻ ORR and 2e⁻ WOR on COF-TP.

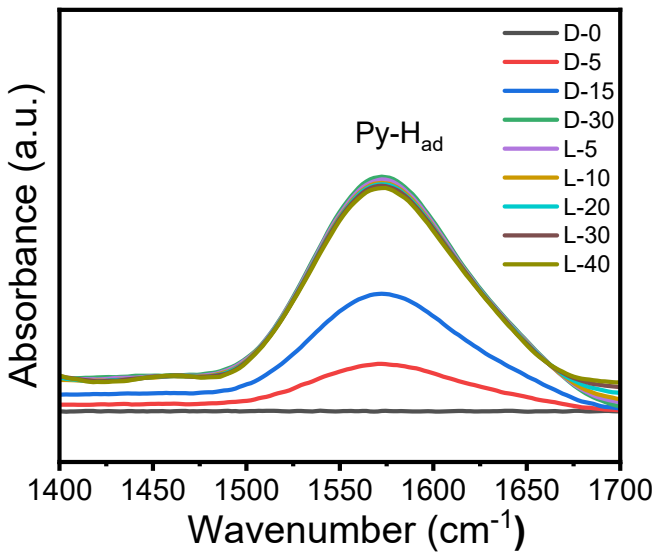

Figure S16 In-situ DRIFTS of probable Py-H_{ad} adsorption signals on COF-BD

Table S1 The comparsion results of COF-BD, COF-TP and other reported results

Photocatalysts	**H_2O_2 production rates**	**Reaction pathways**	**condition**	**References**
COF-NUST-16	1081 μmol g^{-1} h^{-1}	$2e^-$ ORR/$2e^-$ WOR	O_2, λ ≥ 420 nm	10.1016/j.cej.2022.140121
CHF-DPDA	about 600μmol g^{-1} h^{-1}	$2e^-$ ORR	O_2, λ ≥ 420 nm	10.1002/adma.201904433
APFac	1123 μmol g^{-1} h^{-1}	$2e^-$ ORR	O_2, λ ≥ 420 nm	10.1002/anie.202302829
TpAQ-COF-12	420 μmol g^{-1} h^{-1}	$2e^-$ ORR	O_2, λ > 420 nm	10.1016/j.cej.2023.143085
DE7-M	1100 μmol g^{-1} h^{-1}	$2e^-$ ORR	Air, Sunlight	10.1021/jacs.1c09979
DE7-M	2216 μmol g^{-1} h^{-1}	$2e^-$ ORR	O_2, λ > 420 nm	10.1021/jacs.1c09979
BTT-H3	1588 μmol g^{-1} h^{-1}	$2e^-$ ORR/$4e^-$ WOR	Air, λ = 467 nm	10.1038/s41467-025-55894-y
BTT-H2	1359 μmol g^{-1} h^{-1}	$2e^-$ ORR/$4e^-$ WOR	Air, λ = 467 nm	10.1038/s41467-025-55894-y
BTT-H1	1096 μmol g^{-1} h^{-1}	$2e^-$ ORR/$4e^-$ WOR	Air, λ = 467 nm	10.1038/s41467-025-55894-y
BTT-DAB	854 μmol g^{-1} h^{-1}	$2e^-$ ORR/$4e^-$ WOR	Air, λ = 467 nm	10.1038/s41467-025-55894-y
Ald-TTB-TTA	3169 μmol g^{-1} h^{-1}	$2e^-$ ORR	O_2, λ > 420 nm	10.1021/acsami.4c14391
Por-COF-cya	2209 μmol g^{-1} h^{-1}	$2e^-$ ORR	O_2, λ > 420 nm	10.1002/anie.202423205
TTF@Por-COF-cya	6994 μmol g^{-1} h^{-1}	$2e^-$ ORR	O_2, λ > 420 nm	10.1002/anie.202423205

TACOF-1-COOH	3542 μmol g^{-1} h^{-1}	2e^- ORR/4e^- WOR	O_2, λ > 420 nm	10.1002/anie.202408802
COF-N32	605 μmol g^{-1} h^{-1}	2e^- ORR/2e^- WOR	O_2, λ ≥ 420 nm	10.1038/s41467-023-40007-4
CTF-BDDBN	97.2 μmol g^{-1} h^{-1}	2e^- ORR/2e^- WOR	O_2, λ > 420 nm	10.1002/adma.201904433
COF-BD	**5312 μmol g^{-1} h^{-1}**	**2e^- ORR/4e^- WOR**	**O_2, λ ≥ 420 nm**	**This work**
COF-TP	**14480(10 minutes)/6104 (1h) μmol g^{-1} h^{-1}**	**2e^- ORR/2e^- WOR**	**O_2, λ ≥ 420 nm**	**This work**

References

[1] Kresse G. and Furthmüller J, Efficient Iterative Schemes for Ab Initio Total-Energy Calculations Using a Plane-Wave Basis Set, *Phys. Rev. B*, 1996, **54**, 11169–11186.

[2] Perdew J. P., Burke, K. and Ernzerhof M., Generalized Gradient Approximation Made Simple, *Phys. Rev. Lett.*, 1996, **77**, 3865–3868.

[3] Kresse G. and Joubert D., From Ultrasoft Pseudopotentials to the Projector Augmented-Wave Method, *Phys. Rev. B*, 1999, **59**, 1758-1775.

[4] Blöchl P. E., Projector Augmented-Wave Method, *Phys. Rev. B*, 1994, **50**, 17953–17979.

[5] Grimme S., Antony J., Ehrlich S. and Krieg H., A consistent and accurate ab initio parametrization of density functional dispersion correction (DFT-D) for the 94 elements H-Pu, *J. Chem. Phys.*, 2010, **132**, 154104.

[6] Henkelman G., Uberuaga B. P. and Jonsson H., A climbing image nudged elastic band method for finding saddle points and minimum energy paths, *J. Chem. Phys.*, 2000, **113**, 9901-9904.